Title: The role of snow cover on ice regime across Songhua River Basin, Northeast China

Qian Yang[1, 2], Kaishan Song[1, *], Xiaohua Hao[3], Zhidan Wen[2], Yue Tan[1], and Weibang Li[1]

[1]Jilin Jianzhu University, Xincheng Road 5088, Changchun 130118 China; E-Mail: jluyangqian10 @hotmail.com

[2] Northeast Institute of Geography and Agroecology, Chinese Academy of Sciences, Shengbei Street 4888, Changchun 130102 China; E-Mail: songks@neigae.ac.cn;

[3] Northwest Institute of Eco-Environment and Resources, Chinese Academy of Sciences, Donggang West Road 322, Lanzhou 730000, China; E-Mail: haoxh@lzb.ac.cn;

Correspondence to: Song K. S. (songks@neigae.ac.cn)

Abstract: The ice regime has been scarcely investigated in the Songhua River Basin of Northeast China. The regional role and trends of freshwater ice are critical for aquatic ecosystems, climate variability, and human activities. Using ice records of local hydrological stations, we examined the spatial variations of the ice phenology and ice thickness in the Songhua River Basin from 2010 to 2015. We explored the role of snow depth and air temperature on the ice regime. The river ice phenology showed a latitudinal distribution and a changing direction from southeast to northwest. The cluster pattern of yearly maximum ice thickness has been measured by Global and local Moran's I. The high values clustered in the Xiao Higgan Mountain and low values clustered in the Changbai Mountain at the 95% confidence level. The maximum ice thickness over 125 cm was distributed along the ridge of Da Hagan Mountain and Changbai Mountain, and maximum ice thickness occurred most often in February and March. Six Bayesian regression models were built between ice thickness, air temperature, and snow depth in three sub-basins of the Songhua River Basin. The determine R^2 of Bayesian linear regression ranged from 0.80 to 0.95, and root mean square errors ranged from 0.08 to 0.18. Results showed significant and positive correlations between snow cover and ice thickness when freshwater was completely frozen. Rather than by air temperature, ice thickness was influenced by cumulative air temperature of freezing through the heat loss of ice formation and decay.

Keywords. River ice phenology, ice thickness, snow depth on ice, cumulative air temperature of freezing, Bayesian linear regression

1 Introduction

The freeze-thaw process of surface ice of temperate lakes and rivers plays a crucial role in the interactions among the climate system (Yang et al., 2020), freshwater ecosystems (Kwok and Fahnestock, 1996) and the biological environment (Prowse and Beltaos, 2002). The presence of freshwater ice is closely associated with social and economic activities, ranging from human-made structures, water transportation, to winter recreation (Lindenschmidt et al., 2017; Williams and Stefan, 2006). Ice cover on rivers and lakes exerts large forces due to thermal expansion and could cause extensive infrastructure losses to bridges, docks, and shorelines (Shuter et al., 2012). Ice cover on waterbodies also provides a natural barrier between the atmosphere and water. Ice cover also blocks the solar radiation necessary for photosynthesis to provide enough dissolved oxygen for fish, thus can have a negative effect on freshwater ecosystems and, in extreme cases, lead to winter kill of fish (Hampton et al., 2017). Generally, the duration of freshwater ice has shown a declining trend, with later freeze-up and earlier break-up throughout the northern hemisphere. For example, freeze-up has been occurring 0.57 days per decade later and break-up 0.63 days per decade earlier during the periods of 1846-1995 (Beltaos and Prowse, 2009b; Magnuson et al., 2000; Sharma et al., 2019). To evaluate the influence of ice regimes on the regional climate and human environment, and provide helpful information for regional projections of climate and ice-river floods, a robust and quantitative analysis on ice processes is necessary. Despite the growing importance of river ice under global warming, very little work has been undertaken to explain the considerable variation of ice characteristics in Northeast China, where lakes and rivers are frozen for as long as five to six months a year.

The earliest ice record in the literature dates back to 150 years ago throughout the northern hemisphere (Magnuson et al., 2000). Ice development and ice diversity scales have been regarded as sensitive climate indicators. Ice phenology and ice thickness have been studied to gain a deeper understanding of ice processes. At medium and large scales within 25 km, optical remote sensing data are widely used for deriving ice phenology (Šmejkalová et al., 2016; Song et al., 2014), while microwave remote sensing are used to estimate ice thickness and snow depth over ice (Kang et al., 2014; Zhang et al., 2019). Wide-range satellites make it possible to link ice characteristic with climate indices, such as air temperature (Yang et al., 2020) or large-scale teleconnections (Ionita et al., 2018).

Still, their spatial resolutions are too coarse to detect ice thickness and snow depth accurately at local scales. For example, the microwave satellite data of AMSR-E have a spatial resolution of 25 km, but the largest width of the Nenjiang River only ranges from 170 to 180 meters. The spatial resolution limits the application of satellite observations to precisely inverse ice thickness, let alone snow depth.

In terms of point-based measurements, the most commonly used ground observations include fixed-station observations, ice charts, volunteer monitoring and field measurements (Duguay et al., 2015). Ground observations depend on spatial distribution and representation and are limited by the accessibility of surface-based networks. Various models have been implemented to derive ice phenology and ice thickness, such as physically-based models (Park et al., 2016), linear regressions (Palecki and Barry, 1986; Williams and Stefan, 2006), logistic regressions (Yang et al., 2020) and artificial neural networks (Seidou et al., 2006; Zaier et al., 2010). The physically-based models consider the energy exchange and physical changes of freshwater ice and require detailed information and data support, including hydrological, meteorological, hydraulic and morphological information (Rokaya et al., 2020). The reliance on information makes the physically-based model more suitable for small watershed applications within 100 km^2. The empirical model enables it possible to predict the changes in ice regime from limited climate data for larger basin applications (Yang et al., 2020). Ice parameters, such as ice thickness, freeze-up and break-up dates, differ significantly from point to point on a given river (Pavelsky and Smith, 2004), and the uneven distribution of hydrological stations poses an obstacle to spatial investigation and modeling. Sufficient historical ice records are necessary to model ice regime and validate the reliability of remote sensing data.

The ice cover of water bodies experiences three stages: freeze-up, ice growth, and break-up (Duguay et al., 2015). The ice phenology, ice thickness, and ice composition change considerably in different stages. Although air temperature dramatically influences the freeze-thaw cycle of river ice, the effect of snow cover cannot be ignored. Generally, the effect of snow depth on the ice forming process is more significant than the impact of air temperature (Morris et al., 2005; Park et al., 2016). In contrast to these studies, Gao and Stefan (2004) found that air temperature had a more significant effect on ice thickness formation than the snow depth. Furthermore, in situ observations at Russian river mouths where ice thickness decreased had not shown any significant correlation between ice

thickness and snow depth (Shiklomanov and Lammers, 2014). Previous studies analyzed the relationship in view of spatial distributions and ignored the frozen status of ice formation processes. The relative influence of snow depth and air temperature on the freshwater ice regimes in Northeast China deserves more exploration.

To evaluate the influence of the ice regime on the regional climate and human environment, a robust investigation and quantitative analysis on ice regime are necessary, which provides helpful information for projecting future changes in the ice regime. The work is the first to present continuous river ice records of three sub-catchments of the Songhua River Basin from 2010 to 2015 and compared the spatial and temporal changes of ice phenology and ice thickness. The influence of snow cover and air temperature on the ice regime was quantitatively explored among the three sub catchments considering the frozen status of river ice.

2 Materials and methods

2.1 Study area

The Songhua River Basin is located in the middle of Northeast China (Figure 1), and includes Jilin Province, Heilongjiang Province, and the eastern part of Inner Mongolia Autonomous Region. The Songhua River is the third-longest river in China and has three main tributaries: Nenjiang River, Main Songhua River, and Second Songhua River (Khan et al., 2018; Zhao et al., 2018). The basins of the three tributary rivers include Nenjiang Basin (NJ), the Downstream Songhua River Basin (SD), and the Upstream Songhua River Basin (SU) (Figure 1). The Nenjiang River has a length of 1370 km, and the corresponding drainage has an area of 2.55 $\times 10^6$ thousand km^2. The Main Songhua River has a length of 939 km and the downstream catchment of the Songhua River Basin (SD) has an area of 1.86 $\times 10^6$ km^2.The Second Songhua River has a length of 958 km and the upstream catchment of the Songhua River Basin (SU) has an area of 6.19$\times 10^6$ km^2 (Chen et al., 2019; Yang et al., 2018). Temperate and cold temperate climates characterize the whole Songhua River Basin: winter is long and cold; spring is windy and dry. Annual average air temperature ranges between 3 to 5℃, while yearly precipitation ranges from 400 to 800 cm from the southeast to the northwest (Wang et al., 2018; Wang et al., 2015).

[Figure 1 is added here]

2.2 Data Source

2.2.1 Ice phenology

The ice records were obtained from the annual hydrological report, including ice phenology, ice thickness, snow depth on ice and air temperature on bank (Hydrographic bureau of Chinese Ministry of Water Resources, 2010-2015). There existed 50, 35 and 71 hydrological stations in the NJ, SU and SD basins, respectively. Five lake ice phenology were available, and the definitions are listed as below (Duguay et al., 2015; Hydrographic bureau of Chinese Ministry of Water Resources, 2015) :

- Freeze-up start is considered the first day when floating ice can be observed with temperatures below 0 ℃;
- Freeze-up end is the day when a steady ice carapace can be observed on the river, and the area of ice cover is more than 80% in the view range;
- Break-up start is the first day when ice melting can be observed with surface ponding;
- Break-up end is the day when the surface is mainly covered by open water, and the area of open water exceed 20%;
- Complete frozen duration is the ice cover duration when the lake is completely frozen during the winter, from freeze-up end to break-up start.

2.2.2 Ice thickness

We used ice thickness, snow depth, and air temperature from 120 stations for the period ranging from 2010 to 2015, to study changes in ice thickness and establish the regression model described below. 37, 28, and 55 stations were located in the NJ, SU and SD basins, respectively. The hydrological report also provided ice thickness, snow depth on ice, and air temperature on bank every five days from November through April, totaling 37 measurements in one cold season. The yearly maximum ice thickness of the river center and the corresponding DOY were calculated from five-day records. The average snow depth ware derived from the mean of three or four measurements around the ice hole for ice thickness measurement without human disturbance (Hydrographic bureau of Chinese Ministry of Water Resources, 2015). To enhance the performance of the regression model, cumulative air temperature of freezing were derived from air temperature from November to March.

2.3 Data analysis

To start with, we analyzed the spatial pattern and mapped the cluster of rive ice phenology using Kriging and Moran's I. Then, we explored the relationship between the ice regime and the impact factors using correlation analysis. Last but not least, we established the quantitative relationship between ice thickness and snow depth, air temperature based on the Bayesian linear regression.

2.3.1 Kriging

Kriging has been widely used to spatially interpolate in situ measurements of ice phenology (Choiński et al., 2015; Jenson et al., 2007), covering freeze-up start, freeze-up end, break-up start, break-up end and complete frozen duration. The average values of five ice phenology were calculated during the periods from 2010 to 2015 and explored in the Geostatistical wizard of ArcGIS software. The interpolation results exhibited their spatial distribution. We chose the ordinary Kriging method and set variation function as the spherical model. Moreover, isophenes connecting locations with the same ice phenology were also graphed based on interpolation results (C.R. Paramasivam, 2019).

2.3.2 Moran's I

Moran's I is a measure of spatial autocorrelation developed by Patrick Alfred Pierce Moran, and spatial autocorrelation is characterized by a correlation in a signal among nearby locations in space (Li et al., 2020). We calculated the global and Anselin Local Moran's I and of completely frozen duration and ice thickness in ArcGIS software environment. The global Moran's I indicate whether the distribution of regional values is aggregated, discrete or random (Mitchell, 2005). The z-score or p-value indicates statistical significance, a positive Moran's I indicate a tendency toward clustering while a negative Moran's I indicate a tendency toward dispersion (Castro and Singer, 2006).

2.3.3 Bayesian linear regression

Ice thickness had been modelled by air temperature and snow depth using Bayesian linear regression, which has been widely used in hydrological and environmental analyses (Gao et al., 2014; Zhao et al., 2013). Bayesian linear regression treats regression coefficients and the disturbance variance as random variables, rather than fixed but unknown quantities. This assumption leads to a more flexible model and intuitive inferences

(Barber, 2008). The Bayesian linear regression model was implemented through two models: a prior probability model considered the probability distribution of the regression coefficients and the disturbance; a posterior model predicted the response using the prior probability mentioned below. Using k-fold cross validation, we divided the input dataset into 5 equal subsets or folds, and treated 4 subsets as the training set and the remaining as our test set. The performance of the regression model was evaluated using the determination coefficient R^2 and the root mean square error (RMSE).

In this paper, we treated ice thickness on the river bank as the Y data, and snow depth over ice and air temperature as the X data with dataset size of 31. The ice thickness was measured on the riverbank every five days from November to March when the river was completely covered with ice with air temperature below 0℃. Air temperature and cumulative air temperature of freezing were considered in modeling. Additionally, the Pearson correlation was calculated to analyze the relationship among the five ice phenology events and ice-related parameters, including maximum ice thickness, snow depth on ice, and air temperature on the bank (Gao and Stefan, 1999; Williams et al., 2004).

3 Results and discussion

3.1 Spatial variations of river ice phenology

The river ice phenology was analyzed herein, included freeze-up start, freeze-up end, break-up start, break-up end, and complete frozen duration. The hydrological report supplied only one record of river ice phenology each year for all the 156 stations. For each hydrological station, the average values of five river ice phenology were calculated from the ice records from 2010 to 2015 and interpolated by Kriging method to analyze the spatial distribution of river ice phenology.

3.1.1 Freeze-up end and break-up process

Figure 2 illustrates the average spatial distribution of freeze-up start and freeze-up end and the isophenes in the Songhua River Basin of Northeast China from 2010 to 2015. Figure 3 shows the spatial distribution of the break-up start and break-up end. The corresponding statistics are listed in Table 1. Freeze-up start ranged from October 28th to

November 21st with a mean value of November 7th, and freeze-up end ranged from November 7th to December 8th with a mean value of November 22nd. Break-up start ranged from March 24th to April 20th with a mean value of April 9th, and break-up end ranged from March 31th to April 27th with a mean value of April 15th. These four parameters showed a latitudinal gradient: freeze-up start and freeze-up end decreased while break-up start and break-up end increased as the latitude increased, except in NJ. The middle part of NJ had the highest freeze-up start and freeze-up end and decreased to the southern and northern parts. As the latitude decreased, the air temperature tended to increase, leading to later freeze-up and earlier break-up with shorter ice-covered duration; vice versa.

[Figure 2 is added here]

[Figure 3 is added here]

[Table 1 is added here]

3.1.2 Complete frozen duration

Figure 4(a) illustrates the average spatial distribution of complete frozen duration interpolated by kriging and the isophenes in the Songhua River Basin from 2010 to 2015. Complete frozen duration ranged from 110.74 to 163.00 days with a mean value of 137.86 days, increasing with latitude. Interestingly, the isophenes of complete frozen duration had different directionality, increasing from the southeast to northwest, which could also be found in the other parameter. Both freeze-up start and freeze-up end correlated negatively with latitude, with coefficients of -0.66 and -0.53, respectively ($n=156$, $p < 0.001$). Break-up start, break-up end, and complete frozen duration were all positively correlated with latitude with coefficients of 0.48, 0.57, and 0.55, respectively ($n=156$, $p < 0.001$). We built the linear regression equations between the river ice phenology and latitude. As the latitude increased by one degree, freeze-up start and freeze-up end happened 2.56 and 2.32 day early, the break-up start and break-up end arrived 2.36 and 2.37 day late, resulting in 4.48 days decrease in complete frozen duration. This could be explained by the decreasing solar radiation with latitude influencing the ice thaw and melting processes directly.

The Global Moran's I statistic of complete frozen duration was 1.36 with z scores and p value of 2.41 and 0.02, which indicated that likelihood that complete frozen duration showed a clustered pattern was more than 95% for the whole basin. Then Anselin local

Moran's I was calculated to identify statistically significant spatial outliers for each hydrological location in Figure 4(c), and found out that 14 of 156 hydrological stations showed a statistically significant cluster of high values, 17 of 156 showed a statistically significant cluster of low values and 124 of 156 showed no significant cluster at the 95 percent confidence level. Both global and local Moran's I indicated the high values of complete frozen duration clustered along the Xiao Higgan Mountain, and the low values of complete frozen duration grouped in the Changbai Mount.

[Figure 4 is added here]

3.2 Variations of ice thickness

We explored the spatial pattern of ice thickness based on the maximum ice thickness with dataset size of 156 stations and examined the seasonal changes of ice thickness based on the time series with dataset size of 37 days.

3.2.1 Spatial patterns of ice thickness

Figure 5 illustrates the spatial distribution of the yearly maximum ice thickness of the river center and the corresponding DOY. Table 2 summarized the statistical result of maximum ice thickness and the DOY. Maximum ice thickness ranged from 12 cm to 146 cm, with an average value of 78 cm. The maximum ice thickness between 76 and 100 cm accounted for the most significant percentage of 43.33%, followed by 31.67% of maximum ice thickness between 50 and 75 cm. Five stations had maximum ice thickness more exceptional than 125 cm. The DOY of maximum ice thickness had an average value of February 21st, and maximum ice thickness mainly occurred 59 and 40 times in February and March, respectively. Four of the five highest maximum ice thickness greater than 125 cm happened in March, which is consistent with the inter-annual changes in ice development shown in Figure 6. The results suggested that the river ice is always thickest and most steady in February or March, which is the best suitable time for human activities such as ice fishing and entertainment. The ice thickness didn't show the same latitudinal distribution as ice phenology, which suggested that more climate factors should be taken into consideration, such as snow depth and wind.

[Figure 5 is added here]

[Table 2 is added here]

3.2.2 Seasonal changes of ice thickness

Figure 6 displays the seasonal changes of ice development using ice thickness, average snow depth on ice, and air temperature on bank every five days from 2010 to 2015. The variations of ice characteristics differed significantly due to time and location. Among the three basins, the NJ basin had the highest snow depth of -29.15 ± 9.99℃, followed by -25.61 ± 9.02 ℃ in the SD basin, and -22.17 ± 7.33 cm in the SU basin. The SD basin had the highest snow depth of 9.18 cm ± 3.39 cm on the average level, followed by 8.35 cm ± 4.60 cm in the SU basin,, and 8.23cm ± 3.92 cm in the NJ basin,. The changes in daily ice thickness and snow depth had a similar overall trend, while air temperature followed the opposite pattern. Both ice thickness and snow depth increased from November and reached a peak in March, then dropped at the beginning of April. The air temperature showed a distinct trend and reached the bottom in the middle of February, which is earlier than the peaks of maximum ice thickness and snow depth. In Figure 6, the day when ice thickness reached the maximum value was 49, 54 and 49 days later than that when air temperature reached the lowest value in the NJ, SU and SD basin respectively.

[Figure 6 is added here]

3.3 The relationship between ice regime and climate factors

3.3.1 Correlation analysis

Figure 7 displays the correlation matrix between lake ice phenology events and three ground measurements with a dataset size of 120 stations. The lake ice phenology events included freeze-up start, freeze-up end, break-up start, break-up end, and complete frozen duration, and the three ground measurements included yearly mean values of snow depth, air temperature on bank, and maximum ice thickness. The colour intensity and sizes of the ellipses are proportional to the correlation coefficients. Maximum ice thickness had a higher correlation with four of the five indices than snow depth and air temperature on the bank, except with freeze-up start, with which both maximum ice thickness and break-up end had the highest correlation of 0.63 ($p<0.01$, $n=120$). During the freeze-up process, two freeze-up dates had a negative association with maximum ice thickness and snow depth; during the break-up, two break-up dates had a positive correlation with maximum ice thickness and snow depth. The complete frozen duration had a positive correlation with maximum ice thickness and snow depth. The situation of air temperature was

contrary to that of maximum ice thickness and air temperature. Regarding the annual changes, no significant correlation was found between snow depth and five ice phenology events in Figure 7.

[Figure 7 is added here]

Figure 8 shows the bivariate scatter plots between yearly maximum ice thickness and ice phenology with regression equations. The break-up process had a negative correlation with maximum ice thickness, while freeze-up had a positive correlation. Besides, the break-up process had a higher correlation with maximum ice thickness, and the break-up start had the highest correlation coefficients with the maximum ice thickness of 0.65 ($p<0.01$). Complete frozen duration also had a positive correlation with maximum ice thickness of 0.55 ($P<0.01$), which means that a thicker ice cover in winter leads to a delay in melting time in spring. The break-up not only depends on the spring climate conditions but is also influenced by ice thickness during last winter. A thicker ice cover stores more heat in winter, taking a longer time to melt in spring. The limited performance of the regression model could be attributed to the difficulties in determining river ice phenology. Although a uniform specification for ice regime observations was required, the in homogeneities among different stations could not be ignored.

[Figure 8 is added here]

To further explore the role of snow cover, the monthly correlation coefficients between ice thickness and snow depth and ice thickness and air temperature on bank were calculated and listed in Table 3. The correlation coefficients between ice thickness and snow depth increased from November to March and reached a peak of 0.75 in March when ice was thickest. This indicated an increasingly important role of snow depth on ice thickness as the ice accumulated. The higher correlation coefficients between ice thickness and air temperature on bank in November and December revealed that air temperature played a more critical role in the freeze-up process. The positive correlation coefficient between snow depth and ice thickness (Table 3) showed two opposite effects of snow depth during ice development. During the ice-growth process, snow depth protects the ice from cold air and slows down the growth rate of ice thickness. During the ice-decay process, the lake bottom ice stops to grow, and the surface snow or ice melts, and slush forms. The speed of melting depends on the ability to absorb heat, and the slush can absorb more heat, which would promote melting. The slush often existed through multiple freeze/thaw cycles of river ice before completely disappearing. Therefore, the status of river ice could not be neglected when studying the role of snow cover.

[Table 3 is added here]

3.3.2 Regression modelling

We carried out cross-validation for Bayesian linear regression using k-fold method and set K value as 5. For each iteration, a different fold were held-out for testing, and the remaining 4 subsets were used for training. The training and testing were repeated for five iterations. Table 4 listed the R^2 of the training and testing process each iteration. The best Bayesian linear regression was determined when the bias between testing and training regression was the smallest, and the corresponding R^2 were marked as bold and red.

Figure 9 illustrates the scatter plot between measured and predicted ice thickness using Bayesian linear regression in three sub-basins in Northeast China. From Figure 9, the R^2 of Bayesian linear regression ranged from 0.80 to 0.95, and RMSE ranged from 0.08 to 0.18. The model worked best in the SU basin, followed by the NJ and the SD basins. Figure 9 indicates that snow depth outweighed air temperature in terms of the effect on ice thickness, which is consistent with previous studies (Magnuson et al., 2000; Sharma et al., 2019). Moreover, replacing air temperature on bank with cumulative air temperature of freezing enhanced the model performance in all three basins, revealing a more important role of cumulative air temperature of freezing than air temperature. The Bayesian linear regressions just used the field measurement ranging from November to March. During this period, the river surface is completely frozen, and the air temperature that falls below 0℃ promotes the ice growth. In April, air temperature that rose above 0℃ enables the river ice to melt.

[Figure 9 is added here]

The correlation in Figure 7 between air temperature and ice regime was not as significant as in previous studies for several reasons (Gao and Stefan, 2004). Average air temperatures were most commonly calculated over fixed periods at regional scales, for example, as moving averages for specific periods (Pavelsky and Smith, 2004; Yang et al., 2020), which ignored the seasonal changes of air temperature. Our work considered this and established the regression using seasonal time series of ice thickness and air temperature. When building the Bayesian regression equation, the increasing R^2 displayed that the cumulative air temperature of freezing behaved better than the air temperature on bank, which suggested that heat exchanges between river surface and atmosphere dominated the ice process. Heat loss is mainly made up of sensible and latent heat

exchange (Beltaos and Prowse, 2009a; Robertson et al., 1992), which is proportional to cumulative air temperature of freezing during the cooling process. During the complete frozen duration, snow depth, along with wind speed began to influence the heat exchange and ice thickening. Air temperature exerted a lesser effect on spring break-up, which is more dependent on the ice thickness and snow depth. In summary, snow depth dominated the ice process when the river was completely frozen, while cumulative air temperature dominated during the transition process between open water and completely frozen condition.

4 Conclusions

Five river ice phenology indicators, including freeze-up end, freeze-up start, break-up end, break-up start, and complete frozen duration in the Songhua River Basin of Northeast China, have been investigated using in situ measurements for the period 2010 to 2015. The river ice phenology indicators followed the latitudinal gradient and a changing direction from southeast to northwest. The freeze-up start and freeze-up end happened 2.56 and 2.32 day early, the break-up start and break-up end arrived 2.36 and 2.37 days late, resulting in 4.48 days decrease in complete frozen duration. Both Global Moran's I with z score of 1.36 showed that complete frozen duration showed a clustered pattern at the 95% confidence level. The Anselin local Moran's I results showed that the high values of complete frozen duration clustered along the Xiao Higgan Mountain, and the low values of complete frozen duration clustered in the Changbai Mountain. The maximum ice thickness over 125 cm was distributed along the ridge of Da Hagan Mountain and Changbai Mountain, and maximum ice thickness occurred most often in February and March.

.

Based on the analysis of monthly time series, snow cover played an increasingly important role as the ice cover becomes completely frozen. The temporal variability in air temperature was more correlated with the variability in ice phenology than in ice thickness. Six Bayesian regression models were built between ice thickness and air temperature and snow depth in three sub-basins of Songhua River, considering two types of air temperature. Results showed that snow cover correlated with ice thickness significantly and positively during the periods when the freshwater was completely frozen. The cumulative air temperature of freezing behaved better than air temperature when

building the Bayesian regression equation. The results suggested that heat exchanges between the river surface and the atmosphere dominated the ice process, and cumulative air temperature of freezing influenced the thickness is more sensitive indicators of heat loss of ice growth and decay than the air temperature.

This study provided a quantitative investigation of the ice regime in the Songhua River Basin and potential regression models for projecting future changes in the ice regime. Remote sensing data could provide long-term and wide-range information for ice thickness and ice phenology since 1980. The work herein will provide a valuable reference for the retrieval of ice development by remote sensing. Therefore, we plan to use satellite data to enlarge our study scope in our future work.

Author Contribution

Song K.S. and Yang Q. designed the idea of this study together. Yang Q. and Wen Z.D. wrote the paper and analyzed the data cooperatively; Hao X.H. provided valuable suggestions for the structure of study and paper; Li W.B. and Tan Y. exerted efforts on data processing and graphing. This article is a result of collaboration with all listed co-authors.

Competing interest

The authors reported no potential conflict of interest.

Acknowledgments

The research was sponsored by the National Natural Science Foundation of China (41801283, 41971325, 41730104). The anonymous reviewers to improve the quality of this manuscript are much appreciated.

References

Barber, J. J.: Bayesian Core: A Practical Approach to Computational Bayesian Statistics, Journal of the American Statistical Association, 103, 432-433, 2008.

Beltaos, S. and Prowse, T.: River-ice hydrology in a shrinking cryosphere, Hydrological Processes, 23, 122-144, 2009a.
Beltaos, S. and Prowse, T.: River-ice hydrology in a shrinking cryosphere, 23, 122-144, 2009b.
C.R. Paramasivam, S. V.: An Introduction to Various Spatial Analysis Techniques. In: GIS and Geostatistical Techniques for Groundwater Science, Senapathi Venkatramanan, M. V. P., Sang Yong Chung (Ed.), Elsevier, 2019.
Castro, M. C. D. and Singer, B. H.: Controlling the False Discovery Rate: A New Application to Account for Multiple and Dependent Tests in Local Statistics of Spatial Association, Geographical Analysis, 38, 180-208, 2006.
Chen, H., Zhang, W., Nie, N., and Guo, Y.: Long-term groundwater storage variations estimated in the Songhua River Basin by using GRACE products, land surface models, and in-situ observations, Sci Total Environ, 649, 372-387, 2019.
Choiński, A., Ptak, M., Skowron, R., and Strzelczak, A.: Changes in ice phenology on polish lakes from 1961 to 2010 related to location and morphometry, Limnologica, 53, 42-49, 2015.
Duguay, C. R., Bernier, M., Gauthier, Y., and Kouraev, A.: Remote sensing of lake and river ice, 2015.
Gao, B. S. and Stefan, H. G.: Multiple linear regression for lake ice and lake temperature characterisitcs, Journal of Cold Regions Engineering, 13, 59-77, 1999.
Gao, S. and Stefan, H. G.: Potential Climate Change Effects on Ice Covers of Five Freshwater Lakes, Journal of Hydrologic Engineering, 9, 226-234, 2004.
Gao, S., Zhu, Z., Liu, S., Jin, R., Yang, G., Tan, L. J. I. J. o. A. E. O., and Geoinformation: Estimating the spatial distribution of soil moisture based on Bayesian maximum entropy method with auxiliary data from remote sensing, 32, 54-66, 2014.
Hampton, S. E., Galloway, A. W., Powers, S. M., Ozersky, T., Woo, K. H., Batt, R. D., Labou, S. G., O'Reilly, C. M., Sharma, S., Lottig, N. R., Stanley, E. H., North, R. L., Stockwell, J. D., Adrian, R., Weyhenmeyer, G. A., Arvola, L., Baulch, H. M., Bertani, I., Bowman, L. L., Jr., Carey, C. C., Catalan, J., Colom-Montero, W., Domine, L. M., Felip, M., Granados, I., Gries, C., Grossart, H. P., Haberman, J., Haldna, M., Hayden, B., Higgins, S. N., Jolley, J. C., Kahilainen, K. K., Kaup, E., Kehoe, M. J., MacIntyre, S., Mackay, A. W., Mariash, H. L., McKay, R. M., Nixdorf, B., Noges, P., Noges, T., Palmer, M., Pierson, D. C., Post, D. M., Pruett, M. J., Rautio, M., Read, J. S., Roberts, S. L., Rucker, J., Sadro, S., Silow, E. A., Smith, D. E., Sterner, R. W., Swann, G. E., Timofeyev, M. A., Toro, M., Twiss, M. R., Vogt, R. J., Watson, S. B., Whiteford, E. J., and Xenopoulos, M. A.: Ecology under lake ice, Ecol Lett, 20, 98-111, 2017.
Hydrographic bureau of Chinese Ministry of Water Resources: Annual hydrological report: hydrological data of Heilongjiang River Basin. (in Chinese). 2010-2015.
Hydrographic bureau of Chinese Ministry of Water Resources: Specification for observation of ice regime in rivers (in Chinese). 2015.
Ionita, M., Badaluta, C. A., Scholz, P., and Chelcea, S.: Vanishing river ice cover in the lower part of the Danube basin - signs of a changing climate, Sci Rep, 8, 7948, 2018.
Jenson, B. J., Magnuson, J. J., Card, V. M., Soranno, P. A., and Stewart, K. M.: Spatial Analysis of Ice Phenology Trends across the Laurentian Great Lakes Region during a Recent Warming Period, Limnology Oceanography, 52, 2013-2026, 2007.
Kang, K. K., Duguay, C. R., Lemmetyinen, J., and Gel, Y.: Estimation of ice thickness on large northern lakes from AMSR-E brightness temperature measurements, Remote Sensing of Environment, 150, 1-19, 2014.
Khan, M. I., Liu, D., Fu, Q., and Faiz, M. A.: Detecting the persistence of drying trends under changing climate conditions using four meteorological drought indices,

Meteorological Applications, 25, 184-194, 2018.
Kwok, R. and Fahnestock, M. A.: Ice Sheet Motion and Topography from Radar Interferometry, IEEE Transactions on Geoscience Remote Sensing, 34, 189-200, 1996.
Li, R., Chen, N., Zhang, X., Zeng, L., Wang, X., Tang, S., Li, D., and Niyogi, D.: Quantitative analysis of agricultural drought propagation process in the Yangtze River Basin by using cross wavelet analysis and spatial autocorrelation, Agricultural and Forest Meteorology, 280, 107809, 2020.
Lindenschmidt, K.-E., Das, A., and Chu, T.: Air pockets and water lenses in the ice cover of the Slave River, Cold Regions Science and Technology, 136, 72-80, 2017.
Magnuson, J. J., Robertson, D. M., Benson, B. J., Wynne, R. H., Livingstone, D. M., Arai, T., Assel, R. A., Barry, R. G., Card, V., and Kuusisto, E.: Historical Trends in Lake and River Ice Cover in the Northern Hemisphere, Science, 289, 1743-1746, 2000.
Mitchell, A.: The ESRI Guide to GIS Analysis: Vol. 1, Esri Guide to Gis Analysis, 2005. 2005.
Morris, K., Jeffries, M., and Duguay, C.: Model simulation of the effects of climate variability and change on lake ice in central Alaska, USA. In: Annals of Glaciology, Vol 40, 2005, MacAyeal, D. R. (Ed.), Annals of Glaciology-Series, 2005.
Palecki, M. A. and Barry, R. G.: Freeze-up and Break-up of Lakes as an Index of Temperature Changes during the Transition Seasons: A Case Study for Finland, Journal of Applied Meteorology, 25:7, 893-902, 1986.
Park, H., Yoshikawa, Y., Oshima, K., Kim, Y., Ngo-Duc, T., Kimball, J. S., and Yang, D.: Quantification of Warming Climate-Induced Changes in Terrestrial Arctic River Ice Thickness and Phenology, Journal of Climate, 29, 1733-1754, 2016.
Pavelsky, T. M. and Smith, L. C.: Spatial and temporal patterns in Arctic river ice breakup observed with MODIS and AVHRR time series, Remote Sensing of Environment, 93, 328-338, 2004.
Prowse, T. D. and Beltaos, S.: Climatic control of river-ice hydrology: a review, 16, 805-822, 2002.
Robertson, D. M., Ragotzkie, R. A., and Magnuson, J. J.: Lake ice records used to detect historical and future climatic changes, Climatic Change, 21, 407-427, 1992.
Rokaya, P., Morales-Marin, L., and Lindenschmidt, K.-E.: A physically-based modelling framework for operational forecasting of river ice breakup, Advances in Water Resources, 139, 103554, 2020.
Seidou, O., Ouarda, T. B. M. J., Bilodeau, L., Bruneau, B., and St-Hilaire, A.: Modeling ice growth on Canadian lakes using artificial neural networks, Water Resources Research, 42, 2526-2528, 2006.
Sharma, S., Blagrave, K., Magnuson, J. J., O'Reilly, C. M., Oliver, S., Batt, R. D., Magee, M. R., Straile, D., Weyhenmeyer, G. A., Winslow, L., and Woolway, R. I.: Widespread loss of lake ice around the Northern Hemisphere in a warming world, Nature Climate Change, 9, 227-231, 2019.
Shiklomanov, A. I. and Lammers, R. B.: River ice responses to a warming Arctic—recent evidence from Russian rivers, Environmental Research Letters, 9, 035008, 2014.
Shuter, B. J., Finstad, A. G., Helland, I. P., Zweimüller, I., and Hölker, F.: The role of winter phenology in shaping the ecology of freshwater fish and their sensitivities to climate change, Aquatic Sciences, 74, 637-657, 2012.
Šmejkalová, T., Edwards, M. E., and Dash, J.: Arctic lakes show strong decadal trend in earlier spring ice-out, Scientific Reports, 6, 38449, 2016.
Song, C., Huang, B., Ke, L., and Richards, K. S.: Remote sensing of alpine lake water environment changes on the Tibetan Plateau and surroundings: A review, Isprs Journal of Photogrammetry and Remote Sensing, 92, 26-37, 2014.

Wang, M., Lei, X., Liao, W., and Shang, Y.: Analysis of changes in flood regime using a distributed hydrological model: a case study in the Second Songhua River basin, China, International Journal of Water Resources Development, 34, 386-404, 2018.

Wang, S., Wang, Y., Ran, L., and Su, T.: Climatic and anthropogenic impacts on runoff changes in the Songhua River basin over the last 56years (1955–2010), Northeastern China, Catena, 127, 258-269, 2015.

Williams, G., Layman, K. L., and Stefan, H. G.: Dependence of lake ice covers on climatic, geographic and bathymetric variables, Cold Regions Science Technology, 40, 145-164, 2004.

Williams, S. G. and Stefan, H. G.: Modeling of Lake Ice Characteristics in North America using Climate, Geography, and Lake Bathymetry, Journal of Cold Regions Engineering, 20, 140-167, 2006.

Yang, Q., Song, K., Hao, X., Chen, S., and Zhu, B.: An Assessment of Snow Cover Duration Variability Among Three Basins of Songhua River in Northeast China Using Binary Decision Tree, Chinese Geographical Science, 28, 946-956, 2018.

Yang, X., Pavelsky, T. M., and Allen, G. H.: The past and future of global river ice, Nature, 577, 69-73, 2020.

Zaier, I., Shu, C., Ouarda, T. B. M. J., Seidou, O., and Chebana, F.: Estimation of ice thickness on lakes using artificial neural network ensembles, Journal of Hydrology, 383, 330-340, 2010.

Zhang, F., Li, Z., and Lindenschmidt, K.-E.: Potential of RADARSAT-2 to Improve Ice Thickness Calculations in Remote, Poorly Accessible Areas: A Case Study on the Slave River, Canada, Canadian Journal of Remote Sensing, 45, 234-245, 2019.

Zhao, K., Valle, D., Popescu, S., Zhang, X., and Mallick, B.: Hyperspectral remote sensing of plant biochemistry using Bayesian model averaging with variable and band selection, Remote Sensing of Environment, 132, 102-119, 2013.

Zhao, Y., Song, K., Lv, L., Wen, Z., Du, J., and Shang, Y.: Relationship changes between CDOM and DOC in the Songhua River affected by highly polluted tributary, Northeast China, Environmental Science Pollution Research, 25, 25371-25382, 2018.

Tables

Table 1 Summary statistics of ice phenology interpolated by Kriging from 2010 to 2015. The ice phenology indicators included freeze-up start (FUS), freeze-up end, break-up start (BUS), break-up end (BUE), complete frozen duration (CFD). NJ, SD and SU represent the Nenjiang Basin, the downstream Songhua River Basin (SD) and the upstream Songhua River Basin (SU). DOY denotes day of year. Std Dev. denotes standard deviation.

Basins	Statistics	FUS (DOY)	FUE (DOY)	BUS (DOY)	BUE (DOY)	CFD (day)
NJ	**Maximum**	319.14	334.98	110.54	117.61	163.00
	Mean	307.02	324.58	98.65	106.64	139.39
	Minimum	301.41	311.30	84.53	90.40	119.11
	Std Dev.	3.91	5.69	8.16	6.80	13.22
SD	**Maximum**	321.08	334.36	110.01	102.84	154.06
	Mean	313.74	326.70	102.55	97.15	140.86
	Minimum	305.64	316.80	93.22	92.37	125.32
	Std Dev.	2.83	3.13	3.92	2.12	5.69
SU	**Maximum**	325.92	342.09	98.25	114.37	133.62
	Mean	320.39	334.35	91.93	106.43	122.61
	Minimum	313.79	327.68	83.46	95.69	110.74
	Std Dev.	2.34	3.09	3.21	4.24	4.85
Total	**Maximum**	325.92	342.09	110.54	117.61	163.00
	Mean	311.16	326.58	99.25	105.38	137.86
	Minimum	301.41	311.30	83.46	90.40	110.74
	Std Dev.	5.74	5.54	7.17	6.34	11.68

Table 2 The Frequency of yearly maximum ice thickness from November to April. The row represents different year in cold season and the column represents yearly maximum ice thickness with the unit of cm.

MIT / Month	<50	50-75	76-100	101-125	125-150
December	4	1	0	1	0
January	4	4	1	0	0
February	4	25	26	3	1
March	1	3	24	8	4
April	0	2	1	0	0
After April	0	3	0	0	0
Total	13	38	52	12	5

Table 3 Correlation coefficient between maximum ice thickness (MIT) and average snow depth (ASD), and air temperature on bank (BAT) with a dataset size of 120 stations. The asterisk indicates the significant level of correlation coefficients, ** means significant at 99% level ($p<0.01$), and * means significant at 95% level ($p<0.05$).

Correlation Coefficients	November	December	January	February	March
MIT vs. ASD	0.17	0.66*	0.53*	0.59*	0.75**
MIT vs. BAT	-0.90**	-0.80**	-0.55*	-0.30	-0.45

Table 4 The cross-validation of Bayesian linear regression using k-fold method. The R^2 values of training dataset and testing dataset based on the Bayesian regression. Ice thickness was treated as dependent variables, and air temperature, snow depth on ice as independent variables. Air temperature and cumulative air temperature of freezing were considered in the model building.

Basin	Air temperature		Cumulative air temperature	
	Training	Testing	Training	Testing
NJ	0.80	0.99	0.84	0.99
	0.89	0.80	0.90	0.86
	0.84	0.92	0.89	0.82
	0.90	0.56	0.91	0.61
	0.85	**0.91**	**0.89**	**0.89**
SU	0.83	0.92	0.95	0.98
	0.83	0.65	0.96	0.83
	0.81	0.94	0.95	0.99
	0.84	0.79	**0.95**	**0.93**
	0.82	**0.82**	0.94	0.98
SD	0.80	0.96	0.82	0.98
	0.84	0.16	0.86	0.25
	0.81	0.84	0.82	0.87
	0.79	0.97	0.79	0.96
	0.81	**0.80**	**0.82**	**0.83**

Figures

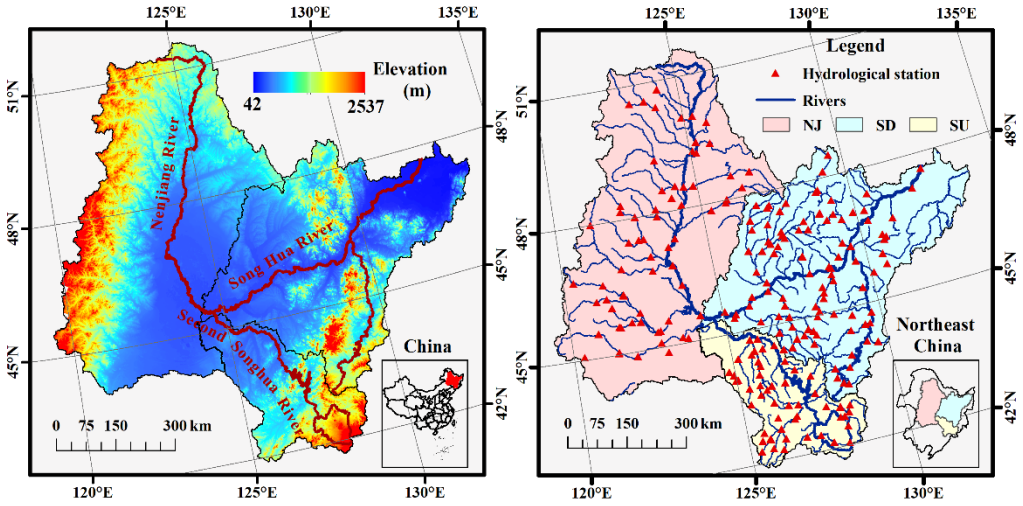

Figure 1 The geographic location of the Songhua River Basin showing (a) the elevation and (b) the location of 156 hydrological stations. The Songhua River Basin includes three sub-basins: Nenjiang River Basin (NJ), downstream Songhua River Basin (SD) and upstream Songhua River Basin (SU). Elevation data are from the Shuttle Radar Topography Mission (SRTM) with spatial resolution of 90 meters.

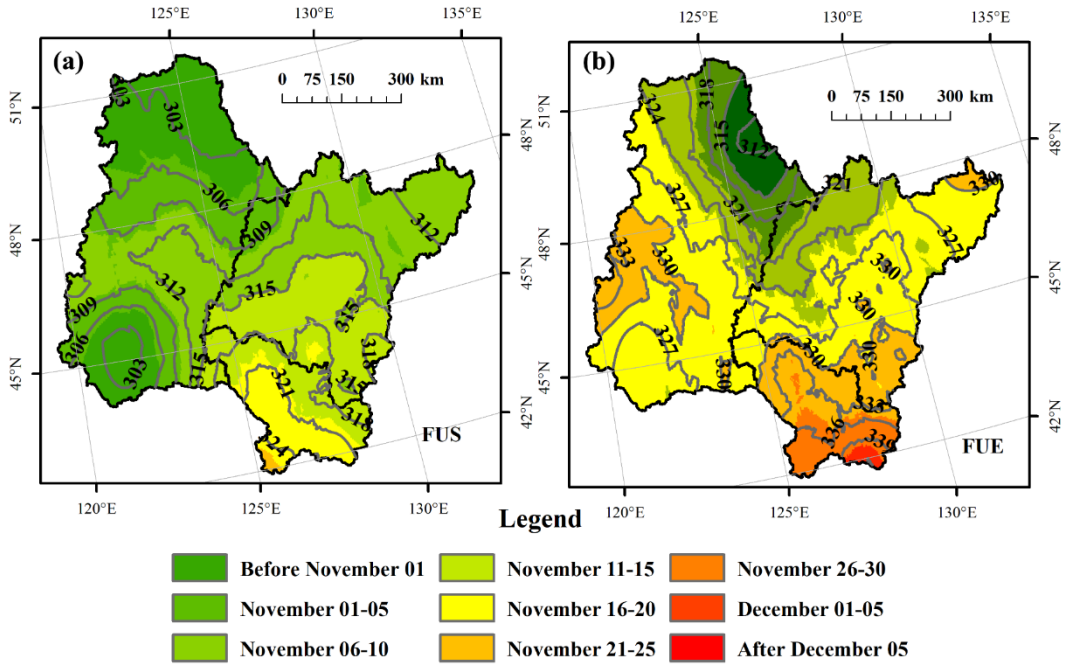

Figure 2 The average spatial distribution of freeze-up start (FUS) (a) and freeze-up end (FUE) (b) in the Songhua River Basin of Northeast China from 2010 to 2015. The number labels indicate the day of year (DOY) of the isophenes.

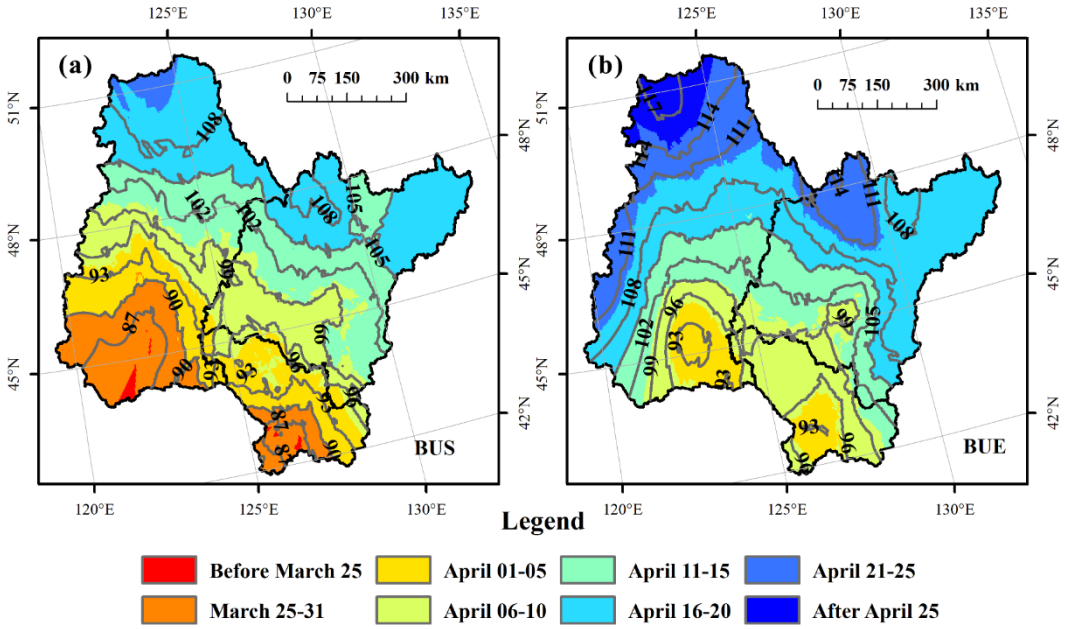

Figure 3 The average spatial distribution of break-up start (BUS) (a) and break-up end (BUE) (b) in the Songhua River Basin of Northeast China from 2010 to 2015. The number labels indicate the day of year (DOY) of the isophenes.

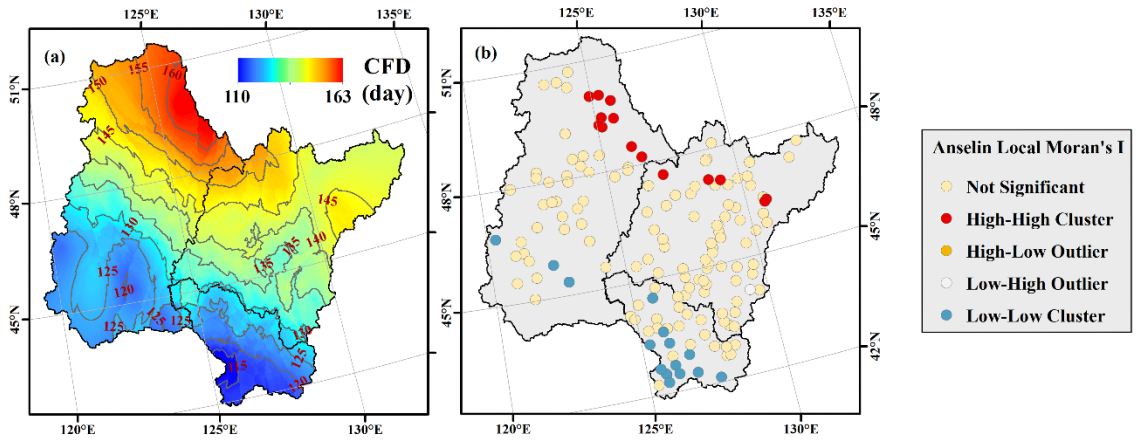

Figure 4 The spatial distribution of complete frozen duration (a) interpolated using Kriging method and Anselin local Moran's I (b) in the Songhua River Basin of Northeast China.

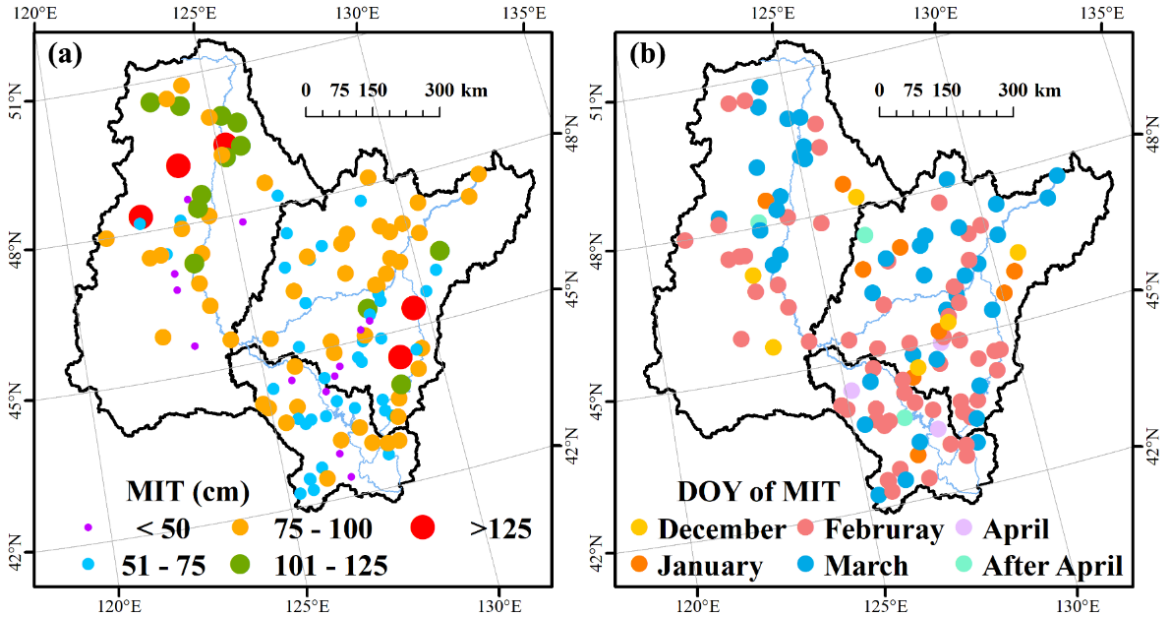

Figure 5 The spatial distribution of yearly maximum ice thickness (MIT) (a) of the river centre and the corresponding date (b).

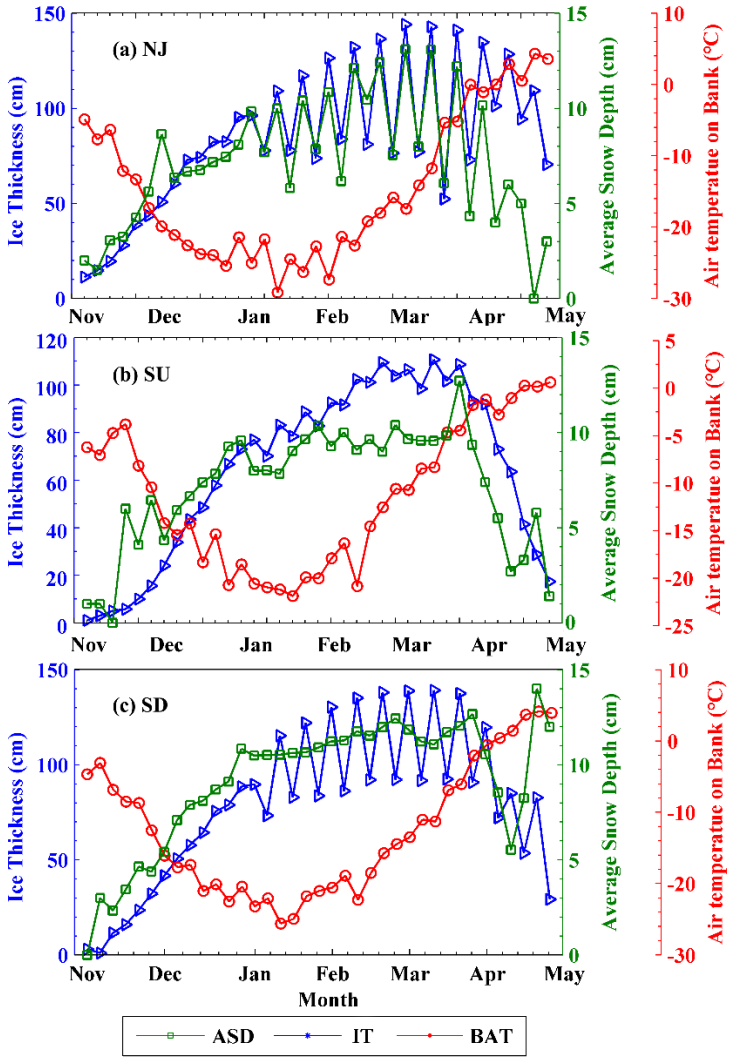

Figure 6 Average seasonal changes in ice thickness (IT), average snow depth (ASD) and air temperature on bank (BAT) from November to April for the period 2010 - 2015.

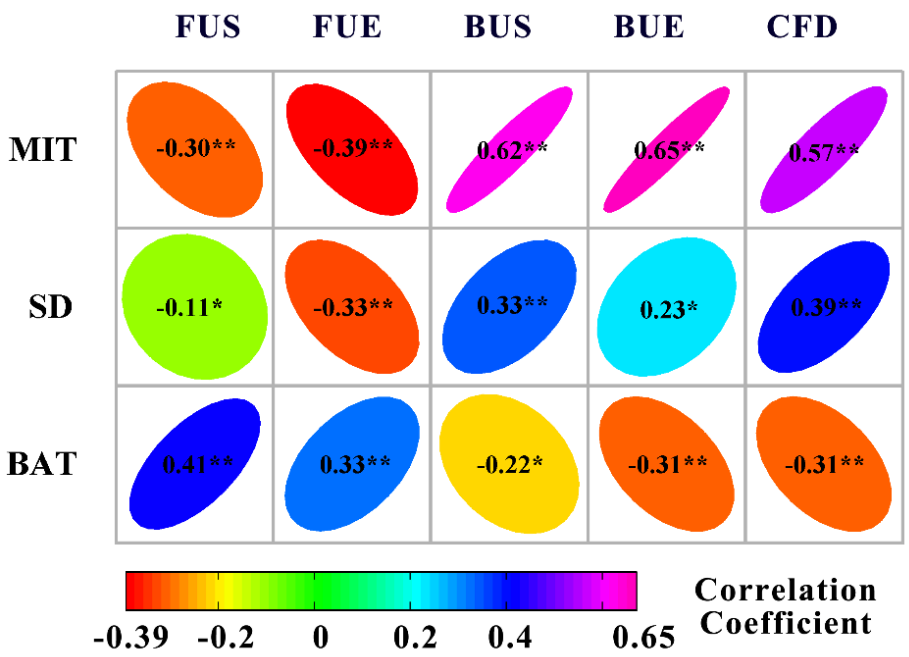

Figure 7 Correlation matrix between maximum ice thickness (MIT), average snow depth (SD) and air temperature on bank (BAT) and lake ice phenology events with data from 120 stations. The asterisk indicates the significance level of the correlation coefficients, ** means significant at 99% level ($p<0.01$), and * means significant at 95% level ($p<0.05$).

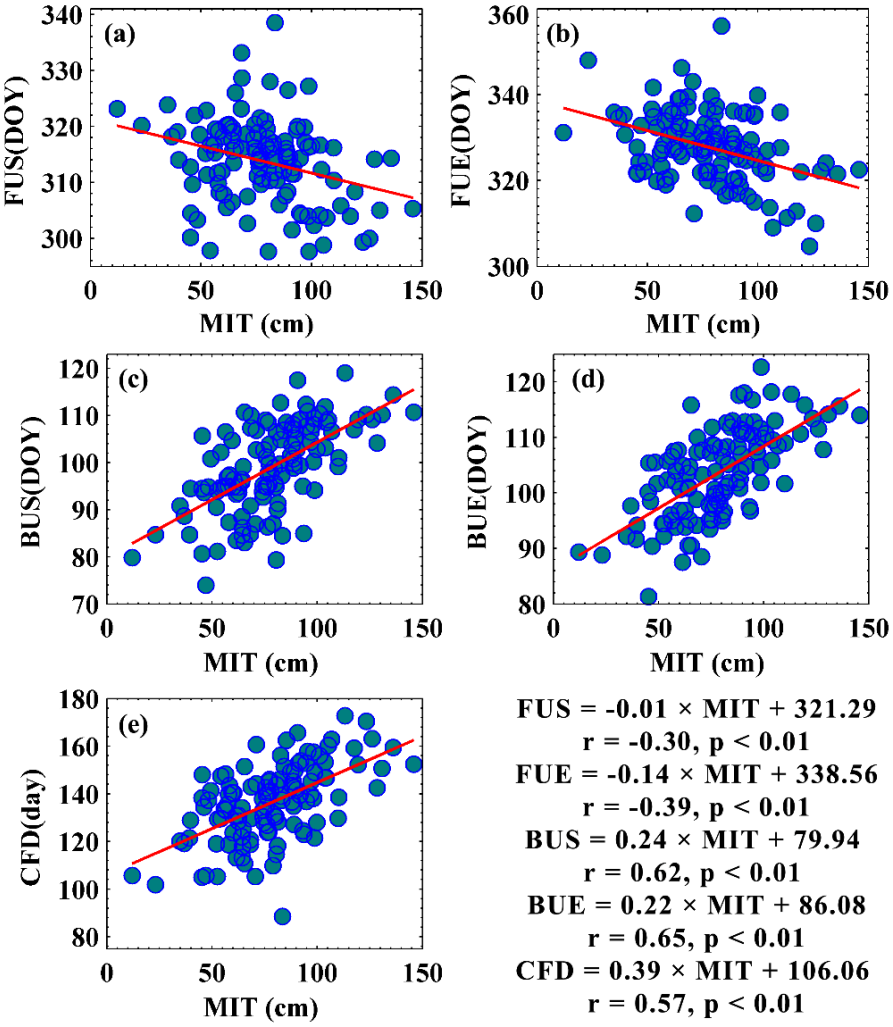

Figure 8 The bivariate scatter plots with linear regression lines between yearly maximum ice thickness (MIT) and ice phenology with dataset size of 120; r and p denote the correlation coefficient and p value of the regression line. The ice phenology events include freeze-up start (FUS), freeze-up end (FUE), break-up start (BUS), break-up end (BUE) and complete frozen duration (CFD).

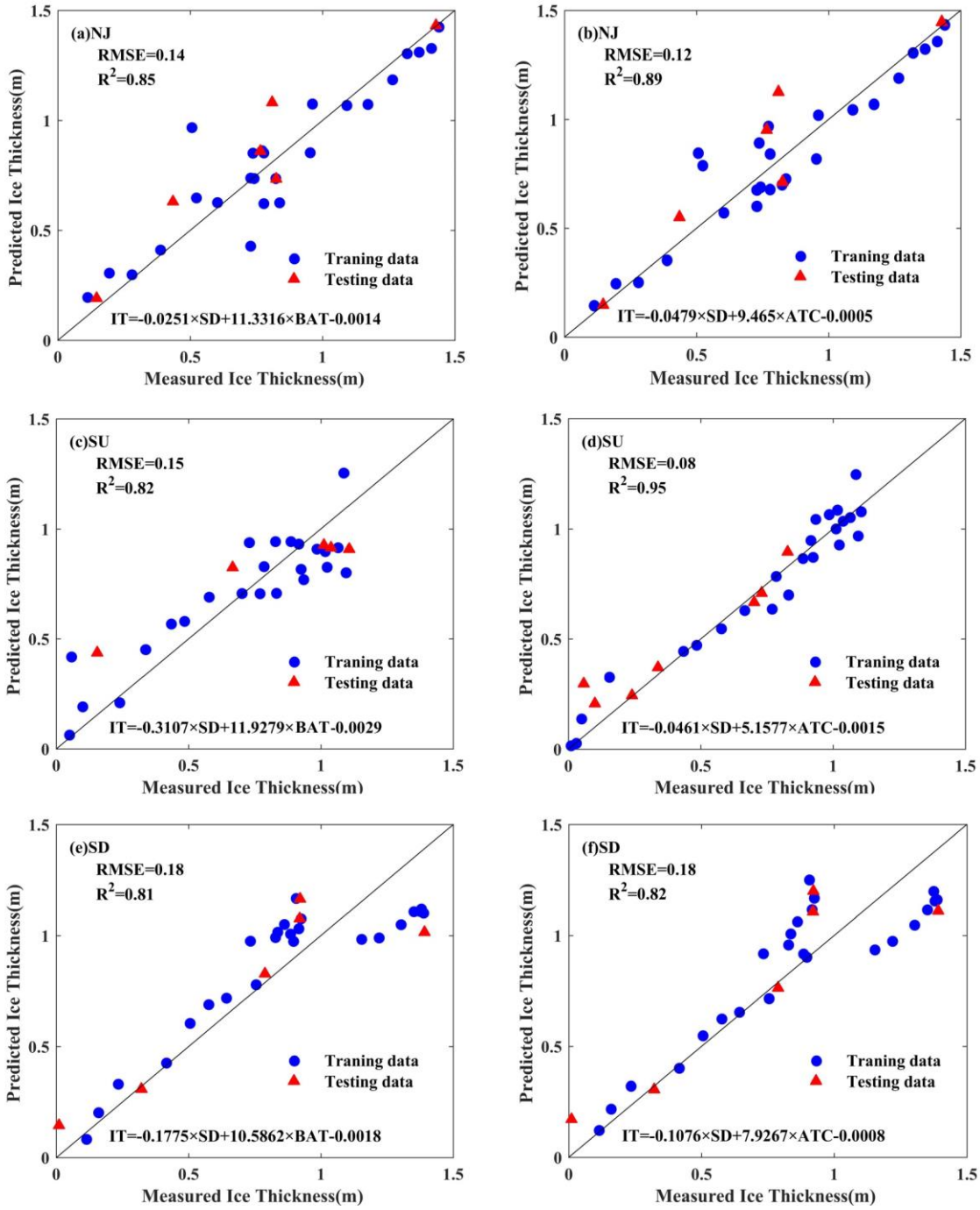

645 Figure 9 Scatter plots between measured and predicted ice thickness using Bayesian linear regression in three sub-basins (NJ: Nenjiang Basin, SU: upstream Songhua River Basin, and SD: downstream Songhua River Basin) in Northeast China. The model treated ice thickness as the independent variable, and snow depth and air temperature as dependent variables. Two types of air temperature were used: BAT represents air
650 temperature on bank; ATC represents cumulative air temperature of freezing.